Effect of Mandrel Rotation on the Accuracy of Computed Temperature Profile during Near Net Shape Forming by Plasma Spraying

Riken R. Patel[1], George S. Dulikravich[2], Arvind Agarwal[1],*

[1]Plasma Forming Laboratory
[2]Multidisciplinary Analysis, Inverse Design, Robust Optimization and Control Laboratory
Department of Mechanical and Materials Engineering
Florida International University
10555 West Flagler Street, EC 3464, Miami, FL-33174

Abstract

Near net shape processing by plasma spray forming (PSF) is a rapid prototyping technique that involves deposition of ceramic coating on the mandrel and its removal as a free-standing structure. This process requires a precise control of the temperature attained by the mandrel during spraying. This article describes the improvement in the accuracy of the temperature prediction of the mandrel by considering the effect of solid rotation inside fluid during conjugate heat transfer. The computation model was modified by incorporating no-slip interface boundary condition instead of tangential slip condition. The transient temperature profiles of the mandrel computed with tangential slip and no-slip interface conditions were validated by experimentally measured temperature profiles. The accuracy of the computed temperature results increased to 95% for no-slip condition as compared to 79% for the tangential slip condition.

* Corresponding Author: Arvind Agarwal, Ph: 305-348-1701, Fax: 305-348-1932
  Email: agarwala@fiu.edu

1. Introduction

Near Net Shape (NNS) fabrication by plasma spray forming (PSF) is an innovative rapid prototyping technique which can be used to fabricate complex shapes for a variety of applications like thin walled zero erosion refractory metal/ceramic nozzles inserts for solid rocket propulsion [1], lightweight space based optics [2], nanostructured composites [3-5] and ultrahigh temperature ceramic components [6-7]. Near net shape forming using PSF technique involves heating/melting of powder and accelerating towards the rotating mandrel for deposition where they rapidly cool forming the desired shape. The positive shape spray-deposited structure is built up on the surface of the mandrel, which has the negative shape. Spray deposited structure could be non-destructively removed from the mandrel, usually by making use of the difference in coefficient of thermal expansion (CTE) between the two components as shown in Figure 1. A wide variety of axi-symmetric, complex shapes and configurations can be manufactured using this technique [3,5,6-8]. The process lends itself especially to refractory metals and ceramics that are generally brittle at room temperature and hard to machine or manufacture into thin walled contoured structure. Most of the above listed work to fabricate thin walled NNS component by PSF has been carried out empirically adopting a trial and approach method. Our research group at Plasma Forming Laboratory (PFL) at Florida international University has attempted to develop a combined experimental and computational approach to fabricate thin walled near net shapes by PSF technique [9,10].
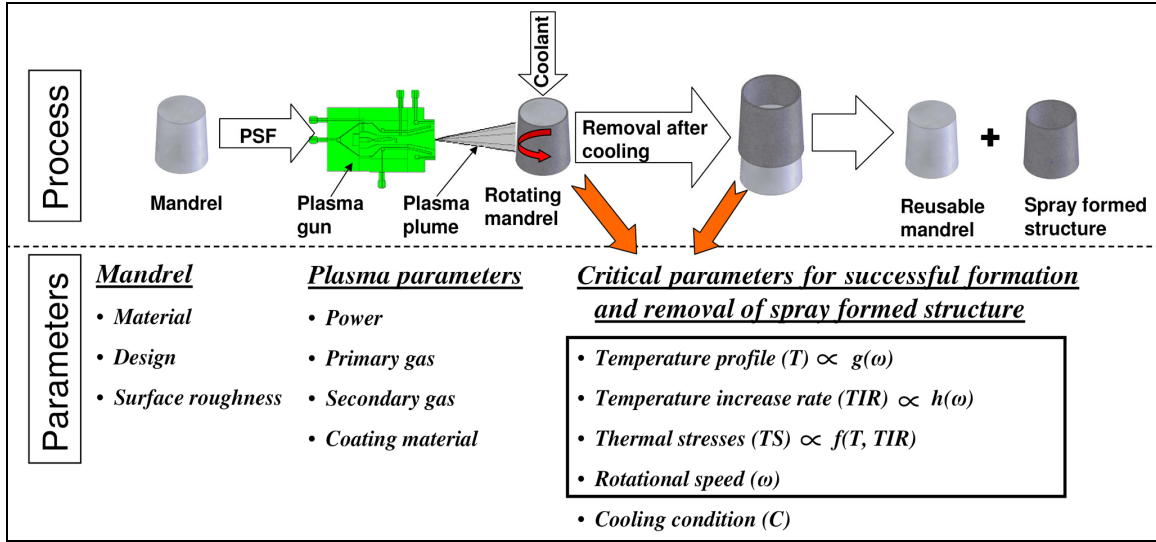
Figure 1. Schematic of near net shape manufacturing by plasma spray forming. The key variables associated with the process are also listed.

The prime challenges with fabricating near net shape structure by PSF are successful "deposition" and 'removability' of the spray formed structure. Removability of the plasma sprayed component from the mandrel largely depends on the heat applied and removed during and after spraying and corresponding overall residual stress induced in the mandrel/coating system. The overall residual stress in ceramic coating is defined as the summation of thermal stress (generated due to temperature mismatch) + quenching stress (25-50 MPa for ceramics) [11,12]. There are several variables that govern the forming and removability of spray deposit as illustrated in Figure 1. These parameters include mandrel material and geometry for a given coating material, plasma parameters, temperature profile generated in the mandrel/coating system during process, corresponding thermal stress, temperature increase rate (TIR) and cooling method during and after spraying. Out of above listed parameters, temperature profile and temperature increase rate (TIR) are most critical parameters for the formation of near net shape

3

structure as thermal stresses depend on temperature [9,10]. If generated overall residual stress is greater than the fracture strength of the coating then it induces cracking during or after spraying. High temperature increase rate (TIR) causes rapid increase in the temperature and may damage mandrel surface. On the contrary, a low TIR may provide the excessive cooled mandrel resulting in poor bonding between successive splats and coating failure during deposition. Thermal stresses generated during the process can be determined based on computed thermal profile and temperature increase rate (TIR). The accuracy of the computed temperature profile and TIR generated in the mandrel is the prime challenge for such a multivariable process.

2. Formulation of the Multivariable Engineering Problem

During near net shape forming by PSF, the rotating mandrel receives heat from the plasma plume and dissipates to the surroundings and to the cooling media as shown in Figure 1. This causes rapid change in the temperature of the mandrel. The process involves complex phenomena of computational fluid dynamics (CFD) and unsteady heat transfer where temperature of the mandrel changes due to fluid-solid interaction. This complex phenomenon can be modeled computationally for better prediction of the temperature and corresponding thermal stresses induced in the mandrel. Mandrel temperature is predicted by solving conjugate problem of CFD and heat transfer by ANSYS CFX™ 11.0 module that utilizes finite volume method.
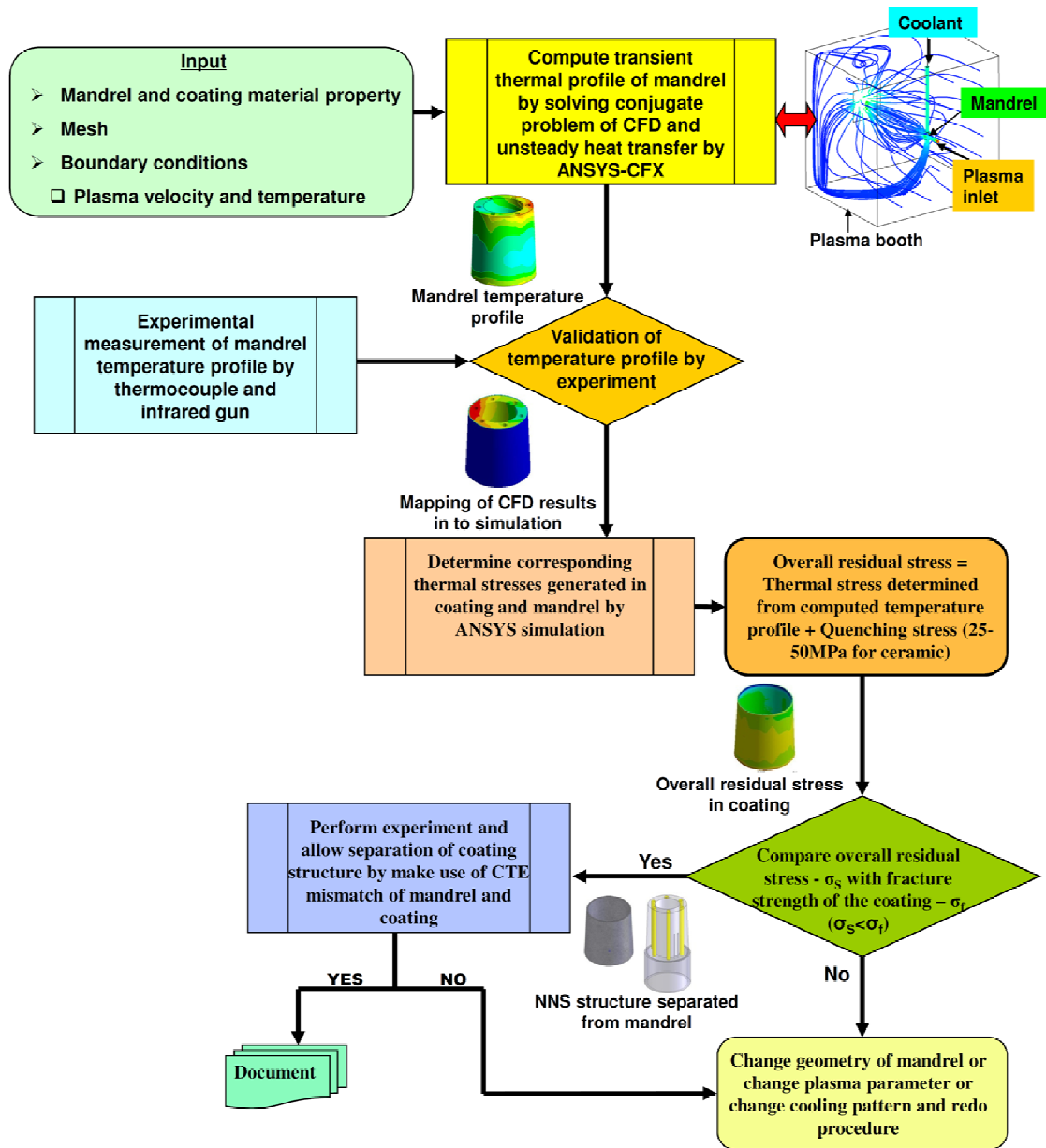
Figure 2. Computational and experimental approaches for developing a protocol for near net shape fabrication by plasma spray forming.

Figure 2 shows a flow chart that summarizes the computational and experimental approach adopted for developing the protocol for near net shape fabrication by plasma spray forming. It is to be noted that entire plasma booth geometry as per actual dimensions (914 mm x 914 mm x 762 mm) was modeled for considering effect of each

constituent on the mandrel temperature as shown in Figure 2 and 3. Computed thermal profile is validated by experimentally measured temperature during plasma spraying. Validated computed temperature profile of the mandrel is mapped in the simulation module. The relative temperature distribution in the coating and mandrel is computed by applying experimentally measured coating temperature (by infrared pyrometer) and by solving steady state problem. Relative temperature distribution is used to compute thermal stress in coating. Thermal stress depends on temperature and temperature increase rate (TIR) whereas mandrel temperature profile and TIR are function of plasma parameters, cooling condition, and mandrel rotation (Figure 1). Conventionally, the solid rotation is considered by rotating the fluid/solid interface without moving the solid. However that approach is useful to derive the information related to flow pattern of the fluid. In the present case the area of interest is the temperature profile of the mandrel (solid) which makes the assumption of mandrel rotation critical. Hence, in present study the computational model was ameliorated by considering the *effect of the mandrel rotation* on its temperature profile. The computational model to predict mandrel temperature profile is developed with two types of fluid/mandrel interface conditions: (i) rotation of fluid/mandrel interface keeping mandrel stationary and (ii) simultaneous rotation of fluid/mandrel interface and the mandrel. The details of both cases are discussed in sections 2.2 and 2.3. The experimental validation was performed using 6061 Aluminum T6 as the mandrel material for the present study as explained in sections 2.1-2.3.

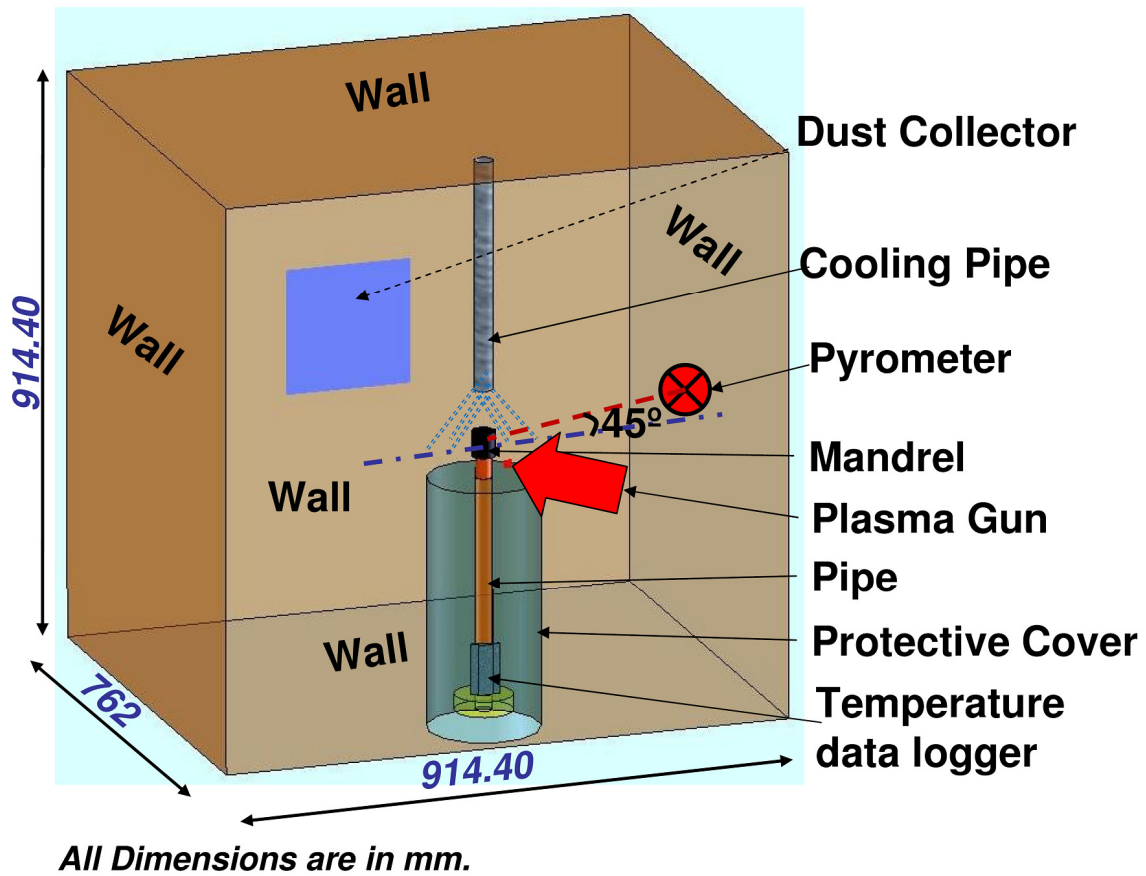## 2.1 Experimental Details and Computational Assumptions

Figure 3 Schematic of the experimental setup for plasma spray forming process inside the spray booth

Plasma spraying facility at Plasma Forming Laboratory (PFL) at Florida International University was utilized for carrying out experiments for this study. The overall arrangement of plasma spraying facility is shown in Figure 3. The rotating chuck is mounted at the bottom of the plasma booth that is connected to a variable speed control motor. Infrared pyrometer was mounted beside the right side wall of the booth. A large hole was made in the wall such that IR pyrometer can focus on the mandrel surface to measure temperature as depicted in Figure 3. Another hole was drilled on the top of the

booth to install cooling fluid pipe for cooling of mandrel. SG 100® plasma gun (Praxair Surface Technologies, Indianapolis, IN), was mounted on a three-axis Velmex gantry robot with stepping motors (Velmex Inc., NY). These motors are communicated by a computer via the VXM stepping motor controllers. A customized program for this study for linear motion of the plasma gun along the mandrel longitudinal axis is utilized. The powder is fed internally to plasma gun at a feed rate of 7.75 g/min using AT1200 powder feeder (Thermach Inc.). Plasma processing parameters utilized for fabrication of near net shape Al_2O_3 parts are as follows: plasma arc with power 32KW, primary gas (standard liters per minutes (slm)- Argon(32.1), secondary gas (slm)- Helium (59.5), carrier gas (slm)- Argon (19.8), and standoff distance -100 mm. It is to be emphasized that there is no well defined protocol for the mandrel design in the literature. The mandrel was designed keeping two factors in consideration: (i) negative of the final desired shape of the spray formed structure and (ii) efficient heat transfer during and after spraying. Hence mandrel was fabricated based on the preliminary *experimental* and *computational* results of temperature distribution and based on our past experience [1-5,7]. Mandrel was designed to improve the heat dissipation by making it hollow and creating cooling channels as shown in Figure 4. This mandrel design enabled access to the inner walls to control cooling rate by supplying coolant from the top. The surface roughness of R_a = 0.67±0.10 micron was maintained for entire research work for ease of removal, the roughness was optimized based on the preliminary experimental results. The evolution of the mandrel design is described elsewhere [9,10] as it is not the focus of the present study.
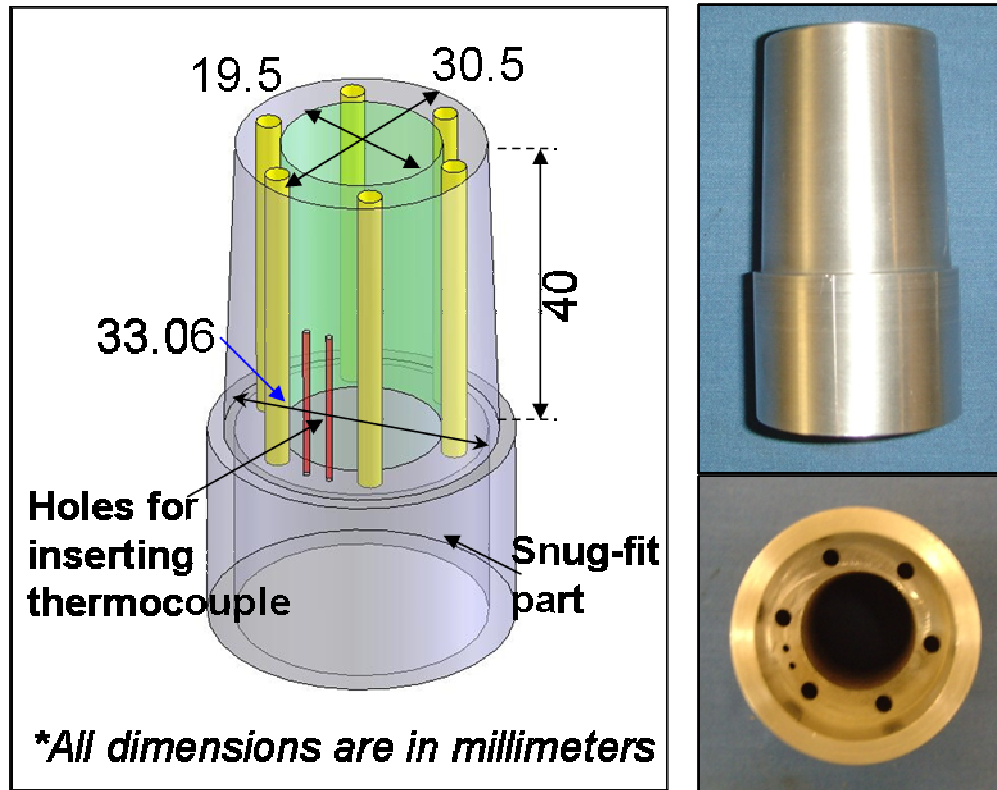
Figure 4. Schematic and photographs of the 6061 aluminum mandrel with cooling channels and holes for inserting thermocouples.

The computational model was developed with the following assumptions.

- All booth walls and cooling pipe were considered as adiabatic.

- The effect of shaft and protective cover (Figure 3) for temperature data logger on the mandrel temperature profile was negligible based on the preliminary computational results and were excluded from the subsequent computational model.

- The plasma gun was considered as stationary in the computational model.

- Mandrel bottom was considered as fixed while computing thermal stress in the coating and mandrel.

Tetrahedral mesh of 1,022,975 elements was generated for the entire plasma booth geometry. Fine mesh with total 355,468 hex dominant elements and 1,016,436 nodes were generated for the stress analysis. Plasma inlet velocity and plasma plume temperature was considered as 240 m/s and 2173 °C, respectively based on the experimental measurements by in-flight diagnostic sensor, AccuraSpray (Tecnar Automation Ltée, QC, Canada). Dust collector suction pressure was defined as 0.85 atm based on on the losses in the duct and efficiency of the dust collector (TORIT model DFO 2-2, IG793813). Cooling air inlet pressure at cooling pipe inlet was defined 1.2 bar based on the experimental measurement. Mandrel rotation of 120 rpm was considered in CFD analysis to account for rotational effect during spraying. Transient simulation was performed up to 120 seconds which is total spraying time including preheating time, to evaluate transient temperature response of mandrel. Two types of solid/fluid interface boundary condition were considered. The details of these interface condition are explained in section 2.2 and 2.3. Solutions converged for mass and momentum, heat transfer and turbulence below the set criteria of residual 1 X 10^{-4} which indicates excellent convergence and hence, accurate results.

2.2 *Computational model with <u>tangential slip</u> at fluid-solid interface*

The computational model was developed using ANSYS CFX 11.0 to predict transient temperature profile generated in the aluminum mandrel with air cooling from the top. The entire geometry of the plasma booth was modeled as per actual dimensions to include the effect of plasma inlet, cooling media and dust collector/exhaust on the

mandrel temperature profile. The detail about the assumptions, geometry modeling, meshing and boundary conditions for computational modeling can be found elsewhere [9, 10]. In the preliminary computational model, the fluid/mandrel interface was considered as rotating while the mandrel (solid domain) was kept stationary as per conventional CFD modeling technique. This was an ideal case of tangential slip boundary conditions as shown in Figure 5. The transient temperature induced in the mandrel was computed considering the fluid/solid interface rotating at tangential velocity ($V_{Tf} = r\omega$) calculated based on the mandrel rotational speed (ω (rpm)) and the distance of interface from the center of rotation (r) while mandrel tangential velocity ($V_{Tm} = 0$). However this computational model with tangential slip did not consider the effect of mandrel rotation on fluid flow pattern.
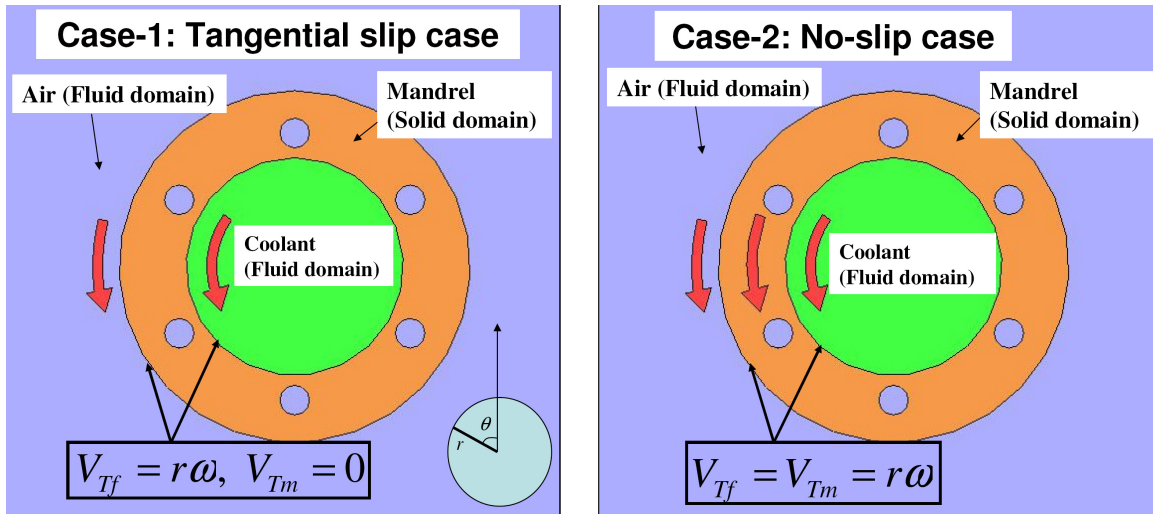

Figure 5. Boundary conditions at the mandrel/fluid interface for Case-1 without considering mandrel rotation and Case-2 with mandrel rotation and β property. V_{Tf} **is the tangential velocity of the fluid at mandrel/fluid interface ,** V_{Tm} **is the tangential velocity of the mandrel,** ω **is the rotating speed in rpm and** r **is the radial distance from the center of rotation.**

2.3   *Computational model with __No-slip__ at fluid solid interface*

The computational model was improved by considering the mandrel (solid domain) rotation at the ω rpm by ANSYS CFX 11.0 β property. The β property allows defining mandrel tangential velocity same as the tangential velocity of fluid/mandrel interface i.e. $V_{Tm} = V_{Tf} = r\omega$. The rotating mandrel setting adds an additional advection term in the computation. This variable setting computes the effect of mandrel rotation on the fluid flow pattern around the mandrel and subsequently, on the mandrel temperature profile. This is typical case of "No-Slip" boundary condition as depicted in Figure 5. The computed temperature profile was compared by carrying out the experiments for the identical process and cooling conditions. Mandrel temperature was measured by quick response thermocouples (TC) KMQSS-020U (Omega Engineering Inc.) inserted at the strategic locations as shown in Figure 6. The details of the experimental arrangement can be found elsewhere [9, 10].
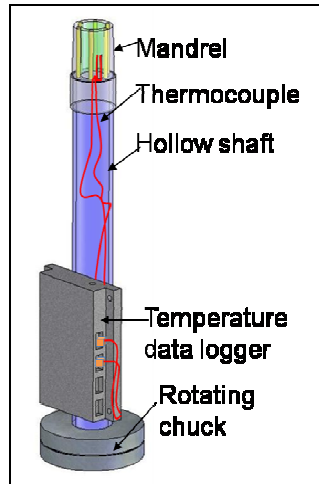

Figure 6. Experimental arrangement of thermocouples inserted in the mandrel for measuring temperature during plasma spray forming.

3. Result and Discussion

This section describes the effect of the mandrel rotation on its transient temperature profile. The computed temperature profile was compared with the experimentally measured temperature profile. The accuracy of the computation in predicting temperature profile is discussed for the tangential slip condition (case-1) and no-slip condition (case-2).

3.1 *Transient temperature profile for <u>Tangential slip</u> interface condition*

The transient temperature profile generated in the aluminum mandrel for spraying time of 120 seconds with air cooling from the top was computed considering tangential slip condition. The mandrel was considered stationary in this computation. The fluid/mandrel interface was considered as rotating at the tangential velocity calculated based on experimental mandrel rotation speed of 120 rpm. The detail about geometry modeling, meshing, boundary conditions, solver and convergence history can be found elsewhere [9, 10].
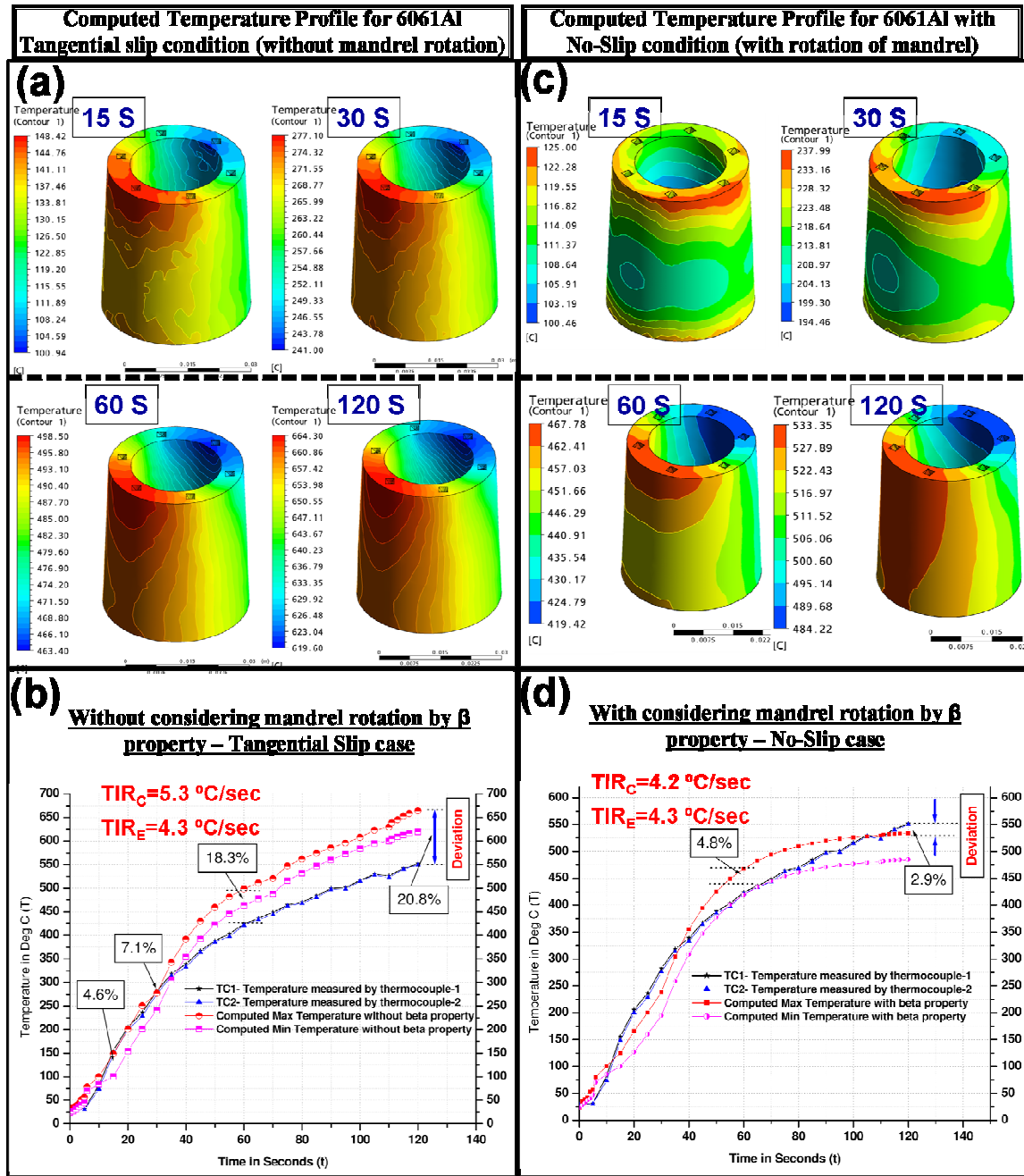
Figure 7. (a) Computed transient temperature profile of 6061Al mandrel with tangential slip condition (b) Comparison of computed temperature profile with experimentally measured temperature for tangential slip (c) Computed transient temperature profile of 6061Al mandrel with no-slip condition (d) Comparison of computed temperature profile with experimentally measured temperature for no-slip.

Computed transient temperature response after 15, 30, 60, 120 seconds of plasma spraying shows gradual temperature increase of aluminum mandrel as depicted in Figure 7 (a). Temperature contours presents unidirectional temperature increase due to the absence of the mandrel rotation effect and stationary plasma gun. The temperature gradient is observed in the direction of heating as the heat input is normal to the mandrel axis. The upper portion of the mandrel shows less temperature as compared to the lower portion due to the external cooling jet provided from the top. Hence, the upper portion of the mandrel has higher degree of cooling which can be observed from the temperature profile of the mandrel. Even though the fluid/mandrel interface was defined rotating but the perimeter of the mandrel facing the plasma remains unchanged as the mandrel was stationary. This affected the accuracy of the predicted mandrel temperature as heating took place only on the one face of mandrel due to plasma plume direction. The deviation of the computed temperature from the experimentally measured value associated with tangential slip interface condition is shown in Figure 7 (b). Computed temperature showed good agreement with the experimental temperature with negative deviation of 4.7% up to 15 seconds of spraying time. The negative deviation increased to 7.1% at 30 seconds. After 30 seconds the computed temperature grew with positive deviation and increased to 18.3% at 60 seconds. As time progresses, the computed mandrel temperature showed tendency of achieving steady state due to unidirectional heating while mandrel is stationary. As a result after 120 seconds the maximum computed temperature had a 20.8% positive deviation from the experimental value. It is emphasized that maximum computed temperature is compared with the experimental temperature to consider worst case scenario as higher temperature induces larger thermal stress in mandrel and coating.

Maximum and minimum computed temperature profile represents the range of temperature achieved in computation. The inaccuracy of computed temperature profile can also be observed from the comparison of temperature increase rate (TIR) for computational and experimental temperature value. TIR was calculated by dividing the temperature difference between before and after spraying by spraying time assuming liner curve (Temperature vs. Time). The computed TIR_C of 5.3 ºC/sec showed deviation of 23.5% from the experimental TIR_E of 4.3 ºC/sec as depicted in Figure 7 (b). Higher TIR corroborates concentrated heating due to assumption of the stationary mandrel and plasma gun condition. This inaccuracy in temperature prediction can be reduced by considering the effect of mandrel rotation in computing the mandrel temperature.

3.2   *Transient temperature profile for <u>No-slip</u> interface condition*

The transient temperature profile of aluminum mandrel was computed with no-slip interface boundary condition where tangential velocity (V_{Tf}) of fluid/mandrel interface was considered same as the tangential velocity of mandrel $V_{Tm} = r\omega$, where ω is the angular speed of the mandrel rotation and r is distance of interface boundary from the center of rotation. The mandrel rotation was defined by ANSYS CFX 11.0 β-property that allows defining mandrel (solid) domain rotation and thus no-slip interface at solid-fluid interface. The simulation was performed keeping all other conditions same as mentioned in section 3.1. Transient thermal profile of aluminum mandrel at 15, 30, 60, 120 seconds with no-slip interface condition was found as depicted in Figure 7 (c). The effect of mandrel rotation on the computed thermal profile is evident from the circumferential distribution of the temperature contour lines. The fluid/mandrel interface

was rotating at the same tangential velocity as mandrel; hence the heat is distributed in the circumferential direction as it occurs during mandrel rotation while plasma spraying. The temperature gradient was found in the circumferential pattern unlike the case of tangential slip where it was unidirectional. The maximum temperature of the mandrel reached to 533 ºC after 120 seconds as shown in Figure 7 (c). Mandrel temperature profile pattern at 120 seconds for no-slip condition was found similar to tangential slip condition case as both the mandrel temperature approached steady state after extended spray time. The steady state implies that temperature profile is not changing with time anymore as shown in Figure 7 (a) and (c). However it is to be noted that computed temperature range for no-slip condition showed better agreement with the experimentally measured value for the entire spray duration as shown in Figure 7 (d). The computed temperature showed a small deviation of 2.9 % at 120 seconds of spraying time. The highest deviation in the computed temperature was 4.8 % at 60 seconds of spray time, which represents the accuracy better than 95%. This improved accuracy of the mandrel temperature prediction is due to the circumferential distribution of the heat in case of no-slip condition unlike unidirectional heating in case of tangential slip. Enhancement of computational model due to no-slip interface condition and accuracy of temperature prediction is also evident from the comparison of experimental and computational TIR. Computed TIR_C of 4.2 ºC/sec showed very good agreement with experimental TIR_E with and accuracy of 98%.

The improved computational model with no-slip interface condition allows accurate prediction of the mandrel temperature profile. Hence thermal stress induced in

coating during spraying can be predicted with a higher accuracy that would result in lesser chance of cracking. This would reduce trial and error approach and number of experiments to be carried out for near net shape forming by plasma spray forming.

4. Conclusions

The accuracy of the computational model to predict the mandrel temperature during plasma spray forming was successfully improved by incorporating the effect of mandrel (solid) rotation inside the fluid domain using β property of ANSYS CFX 11.0. Temperature of the aluminum mandrel was computed with 95% or better accuracy considering no-slip interface boundary condition. Temperature increase rate (TIR) was predicted with 98% accuracy. TIR is an important parameter that governs thermal stress induced in mandrel and coating during and after plasma spray forming process. This improved model can be used for the accurate temperature prediction for any process where solid rotation takes place inside the fluid along with the conjugate problem of fluid flow and unsteady heat transfer.

5. Acknowledgements

References

1. Hickman, R., McKechnie, T., Agarwal, A., 2001. Net Shape Fabrication of High Temperature Materials for Rocket Engine Components. In: 37th AIAA/ASME/SAE/ASEE/Joint Propulsion Conference, Salt Lake City, Utah, USA, AIAA 2001-3435

2. Agarwal, A., McKechnie, T., 2001. Low Cost Fabrication Lightweight Optics, Mirrors and Benches, NAS5-0008, Phase II SBIR Report, NASA Goddard Space Flight Center.

3. Agarwal, A., Seal, S., McKechnie T., 2002. Net Shape Nanostructured Aluminum Oxide Structures Fabricated by Plasma Spray Forming. Journal of Thermal Spray Technology. 12, 350-359.

4. Seal, S., Kuiry, S.C., Georgieva, P., Agarwal, A., 2004. Manufacturing nanocomposite parts: Present status and future challenges. MRS Bulletin, 29 (1), 16-2

5. Viswanathan, T. Laha, K. Balani, Agarwal, A., S. Seal, 2006. Challenges and Advances in Nanocomposite Processing Techniques. Materials Science And Engineering: R: Reports. 54, 5-6, 121-285.

6. Devasenapathi, A., Ng, H.W., Yu, S.C.M., Indra, A.B., 2002. Forming near net shape free-standing components by Plasma spraying. Materials Letters. 57, 882–886.

7. Agarwal, A., McKechnie, T., Starrett, S., Opeka, M.M., 2001. Near Net Shape Forming of Hafnium-Based Ceramic Components: Synthesis and Characterization. In: Elevated Temperature Coatings-4, TMS 2001 Annual Meeting, New Orleans, USA, 301-316.

8. Fang, J.C., Xu, W.J., 2002. Plasma Spray Forming. Journal of Materials Processing Technology. 129, 288-293

9. Patel, R. R., Keshri A. K., Dulikravich G. S., Agarwal A., An Experimental and Computational Methodology for Near Net Shape Fabrication of Thin Walled Ceramic Structures by Plasma Spray Forming submitted to Journal of Materials Processing Technology, Oct 2009 (under review).

10. Patel, R. R., Computational and Experimental Algorithm for Near Net Shape Fabrication of Thin Walled Ceramic Structures by Plasma Spray Forming; M.S. Thesis, Florida International University: Miami, Florida, USA, 2009

11. Kuroda, S., Clyne, T.W., 1991. The quenching stress in thermally sprayed coatings. Thin Solid Films. 200, 49-66.

12. Araujo, P., Chicot, D., Staia, M., Lesage, J., 2005. Residual stresses and adhesion of thermal spray coatings. Surface Engineering. 21, 35-40.